ACS APPLIED MATERIALS & INTERFACES

Research Article

Cite This: ACS Appl. Mater. Interfaces XXXX, XXX, XXX−XXX

www.acsami.org

Improved Ferroelectric Switching Endurance of La-Doped $Hf_{0.5}Zr_{0.5}O_2$ Thin Films

Anna G. Chernikova,[†] Maxim G. Kozodaev,[†] Dmitry V. Negrov,[†] Evgeny V. Korostylev,[†] Min Hyuk Park,[‡] Uwe Schroeder,[‡] Cheol Seong Hwang,[†,§] and Andrey M. Markeev*[,†]

[†]Moscow Institute of Physics and Technology, Institutskii per. 9, 141700 Dolgoprudny, Moscow Region, Russia

[‡]NaMLab gGmbH/TU Dresden, Noethnitzer Strasse 64, 01187 Dresden, Germany

[§]Department of Materials Science and Engineering and Inter-University Semiconductor Research Center, Seoul National University, Seoul 08826, Republic of Korea

Supporting Information

ABSTRACT: $Hf_{0.5}Zr_{0.5}O_2$ thin films are one of the most appealing HfO_2-based ferroelectric thin films, which have been researched extensively for their applications in ferroelectric memory devices. In this work, a 1 mol % La-doped $Hf_{0.5}Zr_{0.5}O_2$ thin film was grown by plasma-assisted atomic layer deposition and annealed at temperatures of 450 and 500 °C to crystallize the film into the desired orthorhombic phase. Despite the use of a lower temperature than that used in previous reports, the film showed highly promising ferroelectric properties—a remnant polarization of ∼30 $\mu C/cm^2$ and switching cycle endurance up to 4×10^{10}. The performance was much better than that of undoped $Hf_{0.5}Zr_{0.5}O_2$ thin films, demonstrating the positive influence of La doping. Such improvements were mainly attributed to the decreased coercive field (by ∼30% compared to the undoped film), which allowed for the use of a lower applied field to drive the cycling tests while maintaining a high polarization value. La doping also decreased the leakage current by ∼3 orders of magnitude compared to the undoped film, which also contributed to the strongly improved endurance. Nonetheless, the La-doped film required a larger number of wake-up cycles (∼10^6 cycles) to reach a saturated remnant polarization value. This behavior might be explained by the increased generation of oxygen vacancies and slower migration of these vacancies from the interface to the bulk region. However, the maximum number of wake-up cycles was less than 0.01% of the total possible cycles, and therefore, initializing the film to the maximum performance state would not be a serious burden.

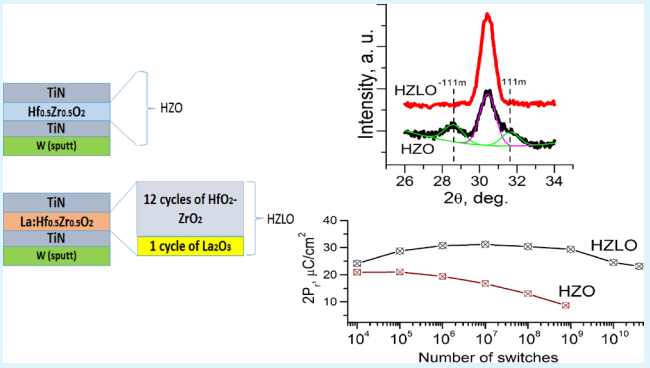

KEYWORDS: *hafnium oxide, multicomponent oxide, thin films, ferroelectricity, nonvolatile memory, atomic layer deposition*

INTRODUCTION

$Hf_{0.5}Zr_{0.5}O_2$ (HZO) thin films are the leading candidate material among the various cation-doped HfO_2-based ferroelectric (FE) thin films for semiconductor memory applications. This is mainly due to the lower processing temperature in the film deposition and annealing of the material (less than 500 °C for annealing is required for crystallization[1−3]) compared to other films, such as Si- or Al-doped HfO_2 films, which require at least ∼800 °C for sufficient crystallization.[4−6] The most feasible film deposition method is atomic layer deposition (ALD), which offers high reproducibility, precise thickness control, and conformal coverage over extreme three-dimensional structures. Moreover, it can be applied not only for growth of functional FE layers but also for CMOS-compatible electrodes, including TiN, Ru, Ir, and so forth.[7,8] ZrO_2 thin films have a lower crystallization temperature compared to HfO_2, making the crystallization of HZO films feasible at such a low temperature. The low processing temperature is critical for integrating the metal−ferroelectric−metal (MFM) structure, where the typical electrode metal is TiN, into the back-end-of-line process, which requires a low temperature (preferably <500 °C). In addition, a higher annealing temperature drives an undesirable phase transition from an orthorhombic phase (o-phase, space group $Pca2_1$), which is the FE phase, to a monoclinic phase (m-phase, space group $P2_1/c$),[2] which largely deteriorates the FE performance. Therefore, low-temperature postdeposition annealing or postmetallization annealing (PMA), which corresponds to annealing after the top electrode (TE) fabrication, is desirable.

Researchers recently reported that annealing at temperatures as low as 400−450 °C could result in crystallization of HZO films and good FE behavior.[9,10] Nevertheless, a minor

Received: October 6, 2017
Accepted: December 28, 2017
Published: December 28, 2017

DOI: 10.1021/acsami.7b15110
ACS Appl. Mater. Interfaces XXXX, XXX, XXX−XXX

formation of the m-phase could not be completely ruled out, which slightly deteriorated the FE performance. Another problem was the relatively low cycling endurance, which is a general problem for this material system. Cycling endurance degradation, which is also called fatigue, corresponds to a decrease of the remnant polarization (P_r) during repeated cycling, while ensuring the exploitation of the full P_r of the film. This issue has been significantly dealt with in conventional perovskite-based FE films, in which the general origin is ascribed to domain pinning by the generation and accumulation of defects, typically oxygen vacancies (V_O), within or at the electrode interface of the film. However, fatigue in HZO (also in other cation-doped HfO_2-based FE films) is usually accompanied by electrical breakdown, which was not the case for conventional perovskite FE films. This can be ascribed to the much higher coercive field (E_c) of these materials (~1 MV/cm) compared to that of conventional perovskites (~0.1−0.2 MV/cm). For a 10 nm thick HfO_2 film, 1 MV/cm of E_c requires 2−3 V of driving voltage, which corresponds to 2−3 MV/cm, to exploit the full P_r values. This driving field is close to the breakdown field (typically, 3.5−5 MV/cm) of the material,[11] so repeated cycling usually induces breakdown before the genuine fatigue performance is evaluated. In contrast to conventional FE materials, the origin of ferroelectricity in HZO films is ascribed to size effects, that is, the lower grain boundary energy of the o-phase compared to that of the m-phase and high kinetic barriers for the phase transitions from the tetragonal phase (t-phase, space group $P4_2/nmc$) and the o-phase to the m-phase.[12−14] In addition, the polarization directions of the crystallized grains in polycrystalline films are not favorably oriented along E_{ext}. Therefore, HZO films have a wide distribution of apparent E_c, which requires a much higher driving field compared to the nominal E_c. A lower E_c is, therefore, desirable. Breakdown could be also accelerated by the leakage current because of the possible impact ionization by electrons and progressive thermal defect generation by Joule heating. This means that a lower leakage current is another critical ingredient to suppress breakdown and to improve endurance.

La^{3+} is a trivalent dopant ion that plays the role of an acceptor with a relatively deep trap position within the band gap in HZO films.[15] HfO_2 and ZrO_2 are vulnerable to reduction, forming V_O, and thus, HZO is also vulnerable, making the undoped film n-type. Therefore, doping HZO films with an acceptor center would shift the Fermi level of the film to the midgap position, which would largely decrease the leakage current with a given relatively low work function of the TiN electrode in this work (~4.5 eV). La is a feasible dopant to induce ferroelectricity in HfO_2 by increasing the tendency for o-phase formation,[16,17] and therefore, a similar effect can be expected in HZO, as will be shown in this work. However, La is also known as an amorphizer in HfO_2,[18,19] so it could adversely interfere with the crystallization if its concentration is not appropriately controlled. In a previous work,[17] the crystallization of La-doped HfO_2 with 2.6 mol % La did not occur after annealing at temperatures lower than 550 °C. Therefore, in this work, a low La content (only 1 mol %) was selected to ensure an early crystallization. The higher tendency of forming the o-phase in HZO films compared to that in HfO_2 renders the adoption of such a low La concentration feasible, which would not be the case in HfO_2.

In this work, the evolution of the structural and electrical properties of a 1 mol % La-doped HZO film (HZLO) was carefully examined and compared to undoped HZO films. It was found that La can decrease the E_c value by ~30% and decrease the leakage current by 3 orders of magnitude compared to the HZO film. These improvements permitted the use of a relatively low driving field during the cycling endurance test, which lowered the chance of breakdown with the help of a lower leakage current. As a result, an endurance cycle up to 4×10^{10} was confirmed without involving detrimental breakdown. Nevertheless, the HZLO film showed a longer wake-up phase because of the generation of more V_O at the interface and slower migration of these vacancies into the film's bulk region. This behavior was carefully monitored by first-order reversal curve (FORC) measurements using the Preisach model.

This work can contribute to the real application of these fluorite-structured FE thin films into semiconductor memory cells, including capacitor-based FE random access memories or FE field-effect transistors. The longer lifetime of the memory cell and lower operation voltage by adopting the HZLO film in this study are critical merits over the cases with undoped HZO films.

EXPERIMENTAL SECTION

Si wafers with previously grown 1 μm thick SiO_2 layers, which provided electrical insulation, were used as substrates. Double metal layers composed of TiN (10 nm)/W (50 nm) served as the bottom electrodes (BE), where the sputtered W layer was used to decrease the series resistance during the electrical measurements (TiN contacts FE films). TiN (20 nm) was grown on the HZLO film to fabricate the TE. Both the BE and TE TiN layers were grown by plasma-assisted atomic ALD (PAALD) using $TiCl_4$ and Ar/NH_3 plasma at a substrate temperature (T_s) of 320 °C (details can be found elsewhere[20]). The low growth temperature of TE TiN in PAALD was helpful to suppress undesired crystallization and grain growth of the FE thin films during TE deposition, which would increase the m-phase portion. A single cocktail source of tetrakis(ethylmethylamino)hafnium and tetrakis-(ethylmethylamino)zirconium mixed in equal mass concentrations and O_2 plasma were used as the Hf/Zr precursor and oxygen source to grow 10 nm thick HZO films at a T_s of 235 °C. The film growth rate was ~0.8 Å/cycle. To dope the HZO film with La, tris(isopropylcyclopentadienyl)lanthanum ($La(iPrCp)_3$) and O_2 plasma were used as the La precursor and oxygen source, respectively, and the growth rate of the La_2O_3 film under the given conditions was ~0.4 Å/cycle. The HZLO film growth was proceeded with pulse−purge cycles consisting of 12 {Hf/Zr single cocktail-purge-O_2 plasma-purge} and 1 {$La(iPrCp)_3$-purge-O_2 plasma-purge}, which resulted in the desired La concentration of 1 mol %. The metal component concentration in the grown films was analyzed by X-ray photoelectron spectroscopy (XPS) with a monochromatic Al Kα (1486.6 eV) X-ray source at a photoelectron take-off angle of 50°. The quantitative cation concentration estimated by XPS was calibrated by Rutherford backscattering spectroscopy. Crystallization annealing was performed using rapid thermal processing (RTP) in an N_2 environment for 30 s at temperatures (T_{ann}) of 400, 450, and 500 °C after the TE deposition.

The structural properties of the annealed HZLO films were examined by grazing-incidence X-ray diffraction (GIXRD) with Cu Kα radiation using an incident angle of 1° (with the presence of the TE TiN layer). The surface microstructures of the HZLO and HZO films were studied by scanning electron microscopy (SEM). To precisely mimic the actual experimental conditions, the HZO and HZLO films were annealed with a TiN TE covering, which was subsequently removed by dipping the sample into H_2O_2 (37%) solution for 15 min at 50 °C before SEM observation. The MFM structures with a TE area of $\sim 2 \times 10^{-5}$ cm^2 were then patterned by photolithography, and the TiN TE was dry-etched using SF_6 plasma. The positive-up-negative-down (PUND) technique based on voltage sweeps and voltage pulses

DOI: 10.1021/acsami.7b15110
ACS Appl. Mater. Interfaces XXXX, XXX, XXX−XXX

was then utilized to measure the FE responses of the MFM capacitors. Particularly, switching current versus electric field (I_s–E) and remnant polarization versus electric field (P_r–E) hysteresis were measured by applying triangular voltage sweeps with frequencies ranging from 100 Hz to 1 kHz. Voltage pulses with different amplitudes and a 600 ns duration (200 ns rise and 200 ns fall times) were utilized to measure the cycle endurance characteristics. Small-signal capacitance–voltage (C–V) measurements were used to estimate the dielectric constant (k) with an ac signal frequency of 10 kHz and amplitude of 50 mV.

RESULTS AND DISCUSSION

First, the influence of La doping on the crystalline structure of the annealed HZLO films was investigated by GIXRD, as shown in Figure 1a, where reference patterns for o-, t-, and c-

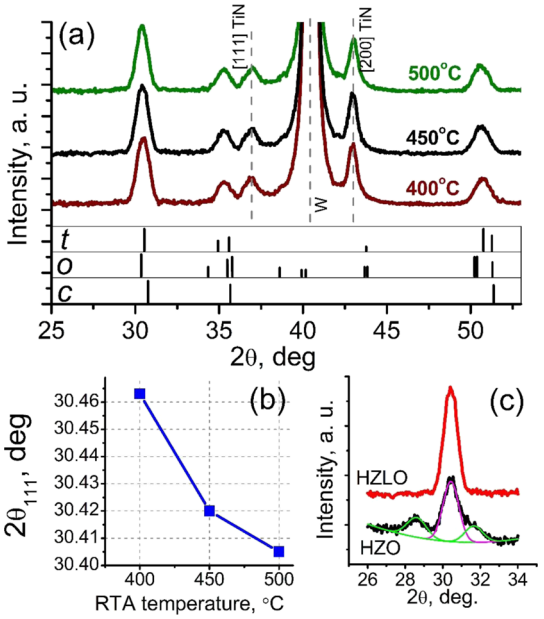

Figure 1. (a) GIXRD spectra collected from the HZLO films after RTP at different temperatures with reference patterns for the o-, t-, and c-phases of HZO; (b) [111] peak position, extracted from GIXRD spectra of the HZLO films, as a function of the RTP temperature; and (c) GIXRD spectra in the 2θ range = 26°–34° of the HZLO and HZO films after RTP at 450 °C.

phases, calculated from the previously reported data,[1,2] were added for clarity. The diffraction peaks at 2θ values of ~30°, 35°, 50°, and 60°–63° suggest that all HZLO films were crystallized even after RTP at 400 °C, despite the well-known amorphization effect of La doping.[18,19] However, it has been reported that the precise determination of the present crystalline phases is quite challenging because the major peaks from the t- and o-phases overlap. Moreover, stabilization of the cubic phase (c-phase, space group $Fm3m$) with very close peak positions cannot be excluded. The most intense diffraction peak near ~30°, which may consist of $[111]_o$, $[111]_t$, and $[111]_c$ reflections, where the subscripts o, t, and c refer to the o-, t-, and c-phases, respectively, may be informative to identify the structural evolution with an increasing RTP temperature. The peak position showed a monotonic shift from ~30.46° to ~30.40° with an increasing annealing temperature from 400 to 500 °C (Figure 1b). According to the appended reference patterns in the lower portion of Figure 1a, this shift may indicate a more preferred o-phase formation with an increasing RTP temperature. Similar shifts were observed previously for other HfO_2-based FE films with an increasing o-phase content.[21] The electrical test results shown later confirm this assumption, where the film after RTP at 400 °C appears to mostly consist of the t-phase.

Second, the positive influence of La doping on the HZO film in achieving the o-phase can be evidently seen from Figure 1c, where the GIXRD patterns of the HZLO and HZO films after RTP at 450 °C are presented in the narrow 2θ range of 26°–34°. The noticeable diffraction peaks at 2θ ~28.5° and ~31.6°, corresponding to the [−111] and [111] reflections of m-phase, are detected for the HZO film, which were not detected for the HZLO film. Additionally, the o-phase peak intensity at 2$\theta \approx$ 30° was higher for the HZLO film. GIXRD spectra fitting, using a peak deconvolution technique assuming a Pearson peak shape, showed that the relative ratio of the integrated area of the peaks corresponding to the m-phase to the sum of all the peak intensities in this region was ~45% for the HZO film, whereas it was negligible for the HZLO film.

It is worth noting that partial formation of the m-phase in PAALD-grown HZO is consistent with previous reports on thermal-ALD-grown HZO.[1−3,22−24] Therefore, it can be concluded that 1 mol % La doping effectively suppresses m-phase formation in HZO, whereas the overall stabilization of the desired o-phase was improved.

It was reported that the phase evolutions in HZO films are largely influenced by the grain size and distribution. Therefore, microstructures of the HZLO and HZO films were analyzed by SEM. Figure 2a,b shows the planar-view SEM images of the mentioned films after RTP at 450 °C, and extracted grain size distributions using the watershed method implemented by the Gwyddion software[25] are presented in Figure 2c. The median grain radii estimated from the Gaussian fitting were ~8.5 ± 0.2 and ~5.9 ± 0.2 nm for the HZLO and HZO films, respectively, and a slight increase in the median grain size occurred with an

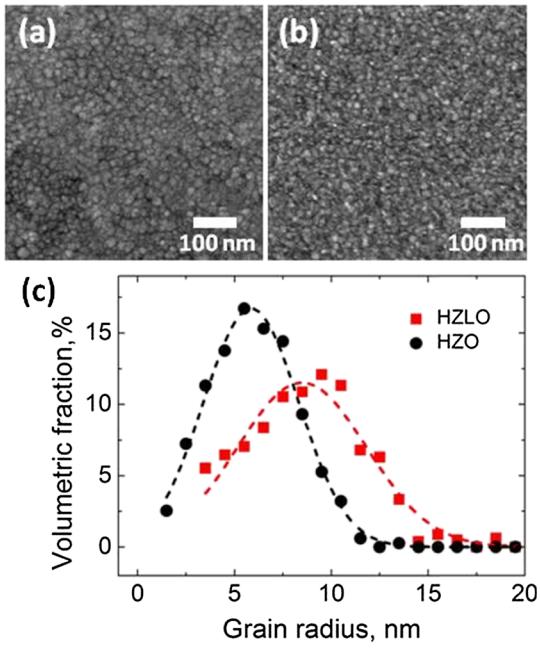

Figure 2. Planar-view SEM images of the HZLO (a) and HZO (b) films after RTP at 450 °C; (c) comparison of grain size distributions of the HZLO and HZO films after RTP at 450 °C analyzed using the watershed method implemented in the Gwyddion software;[25] the lines are the fitting results using Gaussian distributions.

DOI: 10.1021/acsami.7b15110
ACS Appl. Mater. Interfaces XXXX, XXX, XXX–XXX

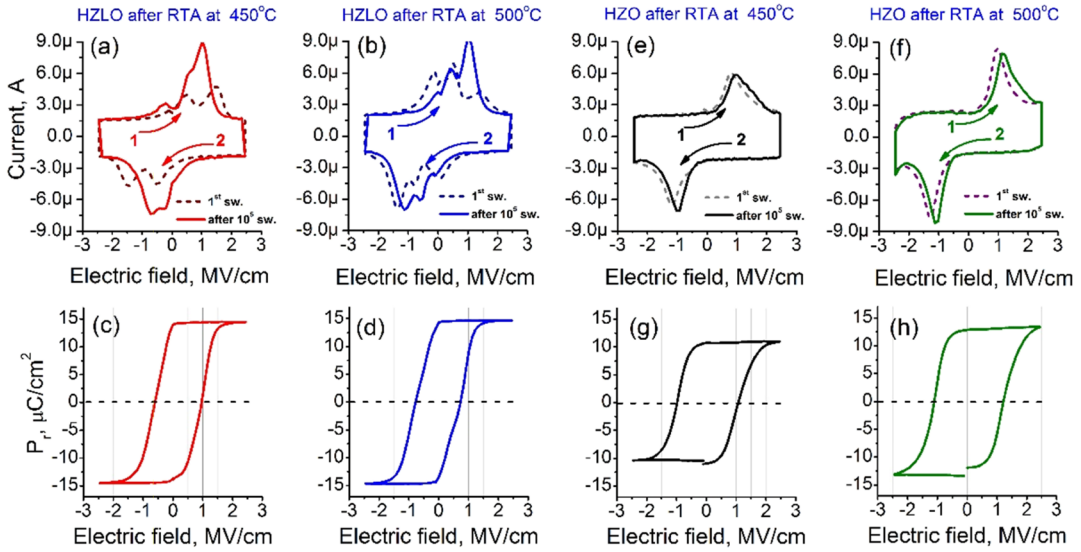

Figure 3. I_s–E curves in response to an applied first voltage sweep and after 10^5 switching cycles for stacks based on HZLO films after RTP at 450 (a) and 500 °C (b) and for stacks based on HZO films after RTP at 450 (e) and 500 °C (f); related P_r–E hysteresis loops extracted by PUND (c,d,g,h).

increase of the RTP temperature (data not shown). The increased grain size in the HZLO film compared to that in the HZO film is not consistent with the previous report on the suppression of the grain growth by the incorporation of La into HZO.[26] The reason for such an abnormal behavior is not clearly understood at this moment, but it is quite notable that the HZLO film contains almost no m-phase despite its larger grain size. This is a demonstration of the positive effect of La doping, which may suppress m-phase formation by decreasing the bulk free energy difference between the m- and o-phases.

Next, the FE properties of the HZLO films were evaluated. Figure 3a,b shows the I_s–E curves for HZLO after RTP at 450 and 500 °C, respectively, in response to the application of a voltage sweep at 100 Hz to the pristine sample (first switch, dotted line) and after 10^5 switching cycles (solid line) with a 2.5 MV/cm amplitude. The resulting P_r–E curves are presented in Figure 3c,d. To make a clear comparison, the same experiments were performed on the HZO film annealed under the same conditions, and the results are shown in Figure 3e,f (for I_s–E) and Figure 3g,h (for P_r–E). The HZO films showed a relatively well-defined single peak in the negative E region in their I_s–E curves for both the pristine (first switch) and awakened states (after 10^5 switching cycles). However, there was certainly an involvement of additional peaks making the peak shape asymmetric in the positive E region. These findings suggest that the film possesses nonuniform E_c values. The peak intensity does not change considerably with increasing switching cycles, suggesting that the wake-up was not significant in this case. The only notable finding is the increased peak height with an increased RTP temperature, suggesting greater o-phase formation, which was confirmed by the higher $2P_r$ value (~25 μC/cm^2) in Figure 3h compared to the $2P_r$ value of ~21 μC/cm^2 in Figure 3g.

By contrast, HZLO films showed quite distinctive I_s–E curves compared to those of the HZO films. There are multiple switching peaks both in positive and negative E regions, suggesting that HZLO films annealed at both temperatures contain several types of grains with different E_c values. Here, the positive and corresponding negative E values, where the observed peaks correspond to the switching field (E_s) and back-switching field (E_{bs}), respectively, and the E_c value can be calculated from eq 1. In an ideal FE film, there should be only one E_s value and one E_{bs} value in the positive and negative fields, of which the absolute magnitude must be identical. If there are multiple values of E_s and E_{bs} and if their magnitudes are not identical, the FE film contains a nonuniform FE performance most likely due to a locally different environment, which also induces a nonuniform field distribution. The internal bias field (E_{bias}) can be calculated from eq 2.

$$E_c = \frac{E_s - E_{bs}}{2} \quad (1)$$

$$E_{bias} = \frac{E_s + E_{bs}}{2} \quad (2)$$

At a RTP temperature of 450 °C, there were primarily two peaks, but for the case of 500 °C RTP, there were primarily three peaks. After the wake-up cycling, the I_s peak height substantially increased for the films exposed to 450 °C RTP, suggesting that considerable wake-up occurred. By contrast, for the case of 500 °C RTP, the overall I_s peak height did not show a notable increase, but the relative intensity between the peaks changed. These findings suggest that the HZLO film had considerable domain pinning in the pristine state, which might be ascribed to the presence of defect centers of La ions and V_O. If the La substitutes Hf or Zr, it may form the effectively negative-charged centers, whereas V_O usually has an effective positive charge, which may pin the domains in the pristine state.

After 10^5 wake-up cycles, the $2P_r$ value was as high as 28 μC/cm^2 for the samples annealed at 450 and 500 °C. This observation is consistent with the lack of m-phase peaks in the GIXRD patterns of HZLO, discussed earlier. The estimated E_c values for both domain groups in HZLO and HZO films after RTP at 450 °C are presented in Table 1 (see Supporting Information section S1 Calculation of the Coercive Fields for Two Domain Groups in HZLO and HZO Films after RTP at 450 °C for more details). Although there are primarily two E_c values for both films, indicating a nonuniform FE performance, the E_c values of HZLO films were lower than those of HZO

DOI: 10.1021/acsami.7b15110
ACS Appl. Mater. Interfaces XXXX, XXX, XXX–XXX

Table 1. Calculated Coercive Fields of the Two Domain Groups of the HZLO and HZO Films Annealed at 450 °C in the Awakened State (after 10^5 Switches)

film	E_{c1}, MV/cm	E_{c2}, MV/cm
HZLO	0.80	0.75
HZO	1.2	0.95

films by ~30%, which explains a significant increase in the $2P_r$ value.

To achieve insight into the observed wake-up phenomenon in HZLO, the well-known FORC measurements within the frame of the Preisach model were utilized,[27] which were applied previously for HfO_2-based FE thin films.[28,29] Here, the switching density ρ was obtained from the numerical solution of the integral equation which connects the total capacitor charge and switching density during the applied voltage ramping. The details of the utilized procedure are presented in the Supporting Information section S2 FORC Measurements.

The HZLO film after RTP at 450 °C was taken as a representative sample and investigated in detail. Because the HZO films did not show notable wake-up, they were not examined using this method. In Figure 4, the switching density (ρ) is plotted as a function of E_{bias} and E_c for different numbers of wake-up cycles, that is, after 10^3, 10^4, 10^5, and 10^6 switches. Here, pulses with a 2.5 MV/cm amplitude were applied for switching. If there were no notable internal E_{bias} and dispersed E_c values among the different regions, a ρ value with a single bright intensity would appear at E_{bias} = 0 and a given E_c. Therefore, the appearance of two bright spots with a rather wide range along the E_c axis and location off of E_{bias} = 0 suggests that there are wide variations in E_c among the different HZLO grains and internal E_{bias}. These bright regions (representing groups of domains) move toward each other during the wake-up process but do not merge completely even after the full wake-up (10^6 cycles). The first group of domains, which are termed "stable" domains, showed a positive E_{bias1} of ~0.5 MV/cm for the maximum ρ from the low cycle numbers, which almost did not change during the wake-up. However, the second group of the domains, which are termed "unstable" domains, initially had an E_{bias2} of ~−0.5 MV/cm and showed noticeable shifts toward the positive E_{bias} direction during cycling before saturating at an E_{bias2} of ~0.1−0.15 MV/cm. At the same time, an increase of the integrated magnitude of ρ with cycling was observed, which is in good accordance with the increased $2P_r$ value during wake-up (shown later). Interestingly, the increased ρ was seen mostly for the unstable domain group, while the stable group appeared to be much less sensitive to cycling. Such behavior of the unstable domains coincides with the previously discussed trend of the disappearance of the built-in field and depinning of the pinned domains during the wake-up cycles.[26,28,29] This effect could be due to defect (V_O) redistribution from the FE/electrode interface toward the bulk, which is also accompanied with a phase transformation from the non-FE phase to the FE phase near the interface during cycling, as suggested by Grimley et al.[30] It is also notable that there are stable domains during the wake-up cycling process in the HZLO film, suggesting that there are FE domains free from the adverse influence of defects and their distribution. The E_c distributions for both groups of domains remained rather wide, that is, from 0.5 to 1.5 MV/cm, during wake-up. These behaviors reveal the complicated FE

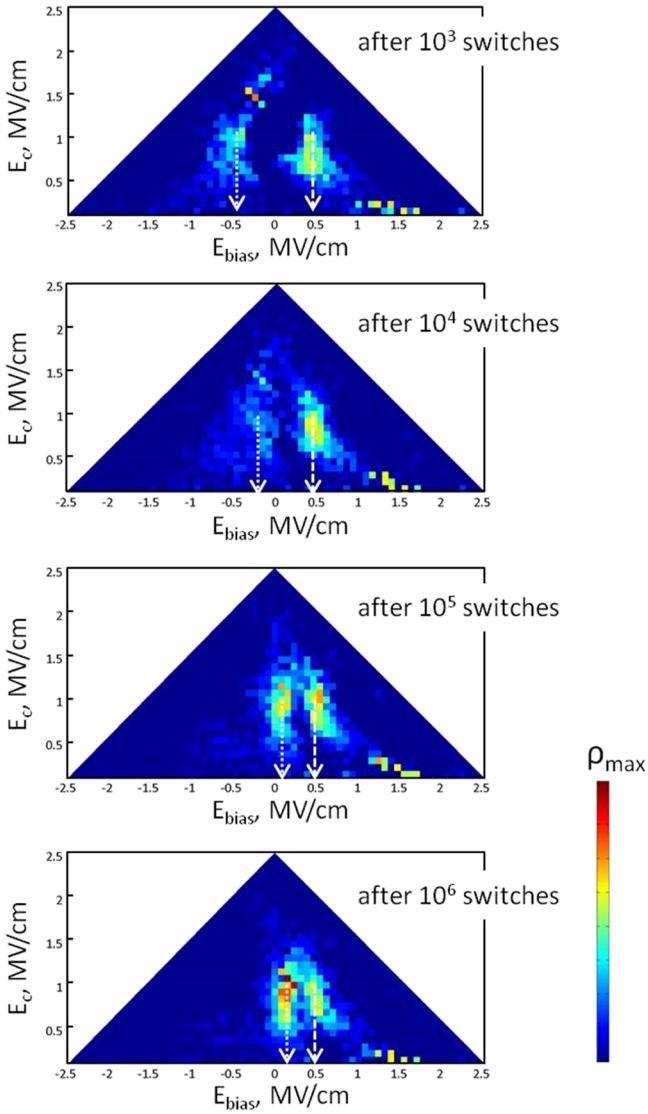

Figure 4. Switching density (ρ) measured from the HZLO-based stack after RTP at 450 °C after 10^3, 10^4, 10^5, and 10^6 switches corresponding to different levels of wake-up. The E_{bias} positions are indicated by the dashed and spot arrows, corresponding to the stable and unstable domain groups, respectively.

domain structure of the HZLO film. The estimated E_{c1} (~0.8 MV/cm) and E_{c2} (~0.75 MV/cm) values in Table 1 almost coincide with the maximum ρ positions in Figure 5 after 10^5 switching cycles.

Next, the cycling endurances of the HZLO and HZO films were examined in detail. Figure 5a demonstrates endurance characteristics of the HZLO-based stacks measured for different field amplitudes. The aforementioned wake-up of $2P_r$ appeared with an increasing number of switching cycles for all the field amplitudes; a near logarithmic growth of $2P_r$ was observed in the wake-up region (i.e., during 10^5 cycles for a 3.0 MV/cm pulse amplitudes and 10^6 cycles for 2.5 and 2.3 MV/cm). By contrast, such a prolonged wake-up was absent in the case of HZO (Figure 5b), suggesting that the prolonged wake-up in the previous case could be ascribed to an effect from La doping. The estimated $2P_r$ values in the awakened state (~10^6 cycles) are ≈38, ≈35, and ≈30 $\mu C/cm^2$ for 3.0, 2.5, and 2.3 MV/cm amplitudes, respectively, which reflect the involvement of different E_c values in different regions (grains), as shown in

DOI: 10.1021/acsami.7b15110
ACS Appl. Mater. Interfaces XXXX, XXX, XXX−XXX

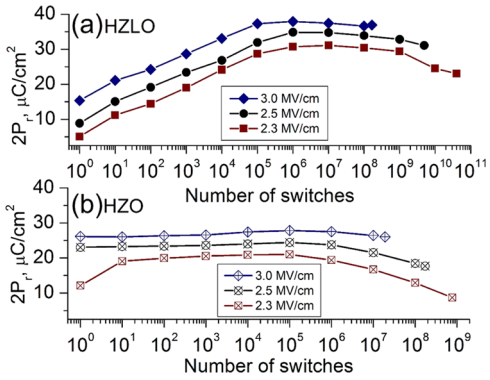

Figure 5. Endurance characteristics of the HZLO (a) and HZO (b) films after RTP at 450 °C measured by PUND with different pulse amplitudes and a constant pulse duration (0.6 μs). After the maximum switching cycles, the samples showed hard breakdown (excluding 2.3 MV/cm case for the HZLO film).

Figure 4. A similar increase in the maximum $2P_r$ with an increasing E_s can also be observed for the HZO film (Figure 5b). However, the relative drop of $2P_r$ in HZLO with a decreased applied electric field from 3.0 to 2.3 MV/cm was ~20%, whereas it was ~25% for HZO.

The improved endurance characteristics for the HZLO film due to its low E_c value were confirmed experimentally. The HZLO film can endure up to ~4×10^{10} cycles for 2.3 MV/cm, while maintaining considerably high $2P_r$ (30 μC/cm^2 up to 10^8 cycles) and displaying no breakdown. The decreased E_c value by La doping allowed for the use of a lower cycling field, which largely mitigates the risk of breakdown. Therefore, genuine fatigue behavior can be observed, and there was a decrease in the $2P_r$ value by 25% at the end of the endurance cycling test. Such degradation might have a similar origin as that for conventional perovskite-based FE materials, that is, domain pinning by defect generation and accumulation.[31] Even for the HZLO film, the adoption of a higher cycling field (3.0 MV/cm) also increases the risk of breakdown, and the film can only be cycled up to 2×10^8 cycles. However, the same field results in a cycle endurance of only 2×10^7 cycles for HZO. The HZO film also showed serious fatigue behavior at ~10^9 cycles even for a lower field (2.3 MV/cm). Therefore, the overall cycle endurance performance was greatly improved by 1 mol % La doping. The reasons for such improvement seem to be twofold: (1) the lowered E_c value, which allowed using a lower cycling field and (2) the lower leakage current. Indeed, as was expected, the dc current density−electric field (J−E) characteristics of the HZLO and HZO films after RTP at 450 °C (the related image is presented in the Supporting Information section S3 dc-IV Characteristics of HZLO and HZO Films) revealed that the HZLO film has a current density considerably lower (in fact, by almost 3 orders of magnitude) than that of HZO at 1 MV/cm. Although identifying the precise origin for such a high J improvement requires further study, such as conduction mechanism analysis and band structure identification by XPS, it is evident that the lower leakage current considerably contributed to the improved reliability and endurance of the HZLO film.

The prolonged wake-up behavior in the HZLO films might be understood from the literature, where the wake-up mechanism has been elucidated. It has been suggested that a very high defect density (mostly V_O) region, especially at the boundary between the FE HfO_2 and TiN electrodes, adversely interferes with FE switching in the pristine state.[32] The presence of such a defective layer results in a built-in E_{bias} in the film, leading to noticeable nonswitched areas inside the film. This is consistent with the observations of the finite E_{bs} and multiple values of E_c in Figure 4. During multiple switching cycles, the diffusion of V_O occurs from the interface to bulk regions, which can considerably diminish the V_O concentration gradient, leading to a relaxation of the built-in field and thus wake-up completion.[28] In this case, the PAALD process for the HZLO film growth ending with La−O layer deposition can lead to a higher defect density at the top interface, as La is known as an effective V_O-generating dopant.[15,33] Thus, many switching

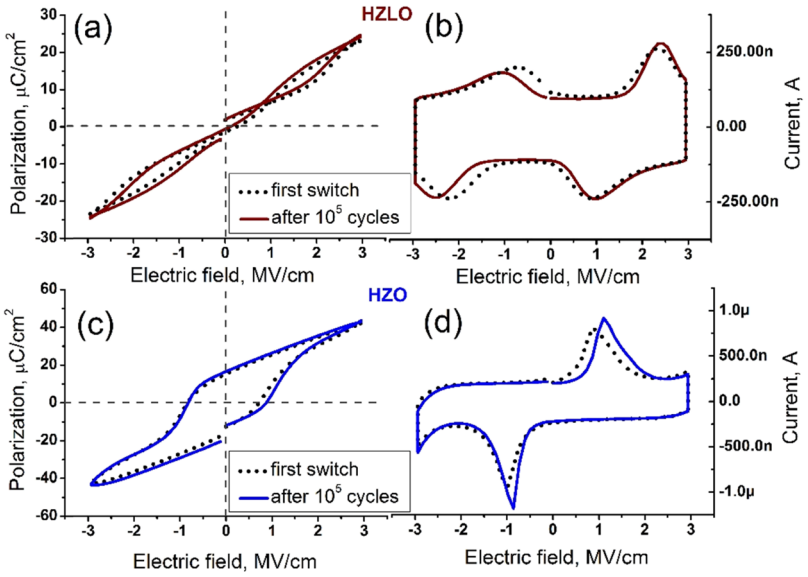

Figure 6. Hysteresis loops with the corresponding current (I_s−E) curves for stacks based on ternary HZLO (a,b)/HZO (c,d) films after RTP at 400 °C in response to the first voltage sweep (first switch) and after 10^5 switches by application of bipolar voltage pulses with a 0.6 μs and 3 MV/cm duration and amplitude, respectively.

DOI: 10.1021/acsami.7b15110
ACS Appl. Mater. Interfaces XXXX, XXX, XXX−XXX

cycles are required to fully wake-up the HZLO film, which was not necessary for the HZO film.

On the other hand, the nonemergence of such a significant wake-up effect in the HZO film might be ascribed to a much higher charge injection compared with the HZLO film case during the wake-up cycles, as could be inferred from the $J-E$ curves shown in Figure S3 of the Supporting Information. The injected charge carriers could pin the FE domains of the HZO film, and the $2P_r$ cannot be increased to the value it should have if there were no charge injections. However, this is unlikely because of the following reason. When the $J-E$ curve of the HZLO film was extrapolated to the E value of 3.0 MV/cm, the J level of the film becomes similar to that of the HZO film at 2.3−2.5 MV/cm. Thus, if the charge injection caused the $2P_r$ suppression, the wake-up should not be observed for the case of the HZLO film at 3.0 MV/cm, which was obviously not the case. Therefore, this possibility can be ruled out.

Finally, the effect of La doping was examined after RTP at 400 °C. Figure 6a,b shows the $P-E$ and I_s-E curves of the HZLO film, respectively. They correspond to an antiferroelectric (AFE)-like behavior, and such behavior did not vary up to 10^5 switching cycles (dotted and solid lines). However, the HZO film, annealed under the same conditions, demonstrated a pure FE response from the first switching cycle (Figure 6c,d) with a $2P_r$ value as high as 25 $\mu C/cm^2$. Such AFE-like behavior of HZLO after RTP at 400 °C may be related to a t-phase formation, which is consistent with the GIXRD spectra presented in Figure 1. Indeed, it has been suggested previously that reversible t−o field-induced transformation can account for the AFE-like behavior.[32] Figure 7 shows the variation of the k value of the HZLO film estimated from the $C-V$ measurements, as a function of the RTP temperature. Here, k values were taken outside the switching regions, that is, at 2.5 MV/cm, to represent only the linear dielectric contribution. The k value was ~38 at 400 °C and decreased to ~33 at 450 and 500 °C. It is well-known that higher-symmetry crystalline phases of HfO_2 are characterized by higher k values. For example, $k \approx 30$ and $k \geq 35$ have been reported for the o- and t-phases, respectively, in $Hf_{0.5}Zr_{0.5}O_2$ thin films.[1,2] Therefore, the observed trend in Figure 7 is consistent with the assumption of a higher t-phase fraction after the RTP at 400 °C. Therefore, activation by La doping for improving the FE performance requires a PMA temperature of at least 450 °C.

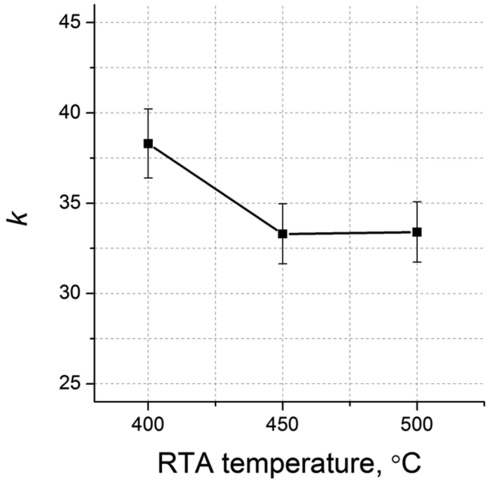

Figure 7. k values of the HZLO film as a function of the RTP temperature in the temperature range of 400−500 °C.

CONCLUSIONS

In conclusion, the advantages of 1 mol % La doping into a PAALD HZO (Hf/Zr = 1:1) film were examined. At RTP temperatures of 450 and 500 °C, the HZLO film showed no formation of the m-phase, which was not the case for the HZO film, and displayed considerably improved FE performances. Interestingly, the HZLO film showed a slightly larger grain size compared to the HZO film, suggesting that the bulk free energy difference between the FE o-phase and non-FE m-phase decreased after La doping. Furthermore, the E_c value of the HZLO film was lower than that of the HZO film by ~30%, and the dc leakage current density was also improved by approximately 3 orders of magnitude compared to HZO. These two effects can be positively combined to strongly enhance the cycle endurance of the HZLO film because the lower E_c permits the use of a lower driving field while maintaining a sufficient $2P_r$ value. This effect considerably lowered the risk of breakdown. The lower leakage current also contributed to a diminished breakdown risk. As a result, the HZLO film endured up to 4×10^{10} cycles at a cycling field of 2.3 MV/cm without breakdown, whereas the HZO film showed deteriorated performance by greater than 10 times. Nonetheless, increased defect generation at the interface by La doping induced much longer wake-up cycling (up to 10^6 at a 2.3 MV/cm cycling field). However, this portion was lower than 0.01% of the entire life cycle (>10^{10}), and therefore, wake-up can be quickly performed before actual device use.

ASSOCIATED CONTENT

Supporting Information

The Supporting Information is available free of charge on the ACS Publications website at DOI: 10.1021/acsami.7b15110.

Calculation of the coercive fields for two domain groups in HZLO and HZO, FORC measurements, and DC-IV characteristics of HZLO and HZO films (PDF)

AUTHOR INFORMATION

Corresponding Author

*E-mail: markeev.am@mipt.ru.

ORCID

Min Hyuk Park: 0000-0001-6333-2668
Uwe Schroeder: 0000-0002-6824-2386
Cheol Seong Hwang: 0000-0002-6254-9758
Andrey M. Markeev: 0000-0001-6777-5706

Notes

The authors declare no competing financial interest.

ACKNOWLEDGMENTS

ALD growth of the HZLO and HZO films and their electrical property investigations were supported by the Russian Science Foundation (project no. 14-19-01645-P) using equipment at the MIPT Shared Facilities Center supported from the Ministry of Education and Science of Russian Federation (grant no. RFMEFI59417X0014). Structural investigations of the mentioned films were supported by the Moscow Institute of Physics and Technology and Russian Academic Excellence Project 5-100 (contract no. 19VP/2017).

DOI: 10.1021/acsami.7b15110
ACS Appl. Mater. Interfaces XXXX, XXX, XXX−XXX

REFERENCES

(1) Müller, J.; Böscke, T. S.; Schröder, U.; Mueller, S.; Bräuhaus, D.; Böttger, U.; Frey, L.; Mikolajick, T. Ferroelectricity in Simple Binary ZrO_2 and HfO_2. *Nano Lett.* **2012**, *12*, 4318−4323.

(2) Park, M. H.; Kim, H. J.; Kim, Y. J.; Lee, W.; Moon, T.; Hwang, C. S. Evolution of phases and ferroelectric properties of thin $Hf_{0.5}Zr_{0.5}O_2$ films according to the thickness and annealing temperature. *Appl. Phys. Lett.* **2013**, *102*, 242905.

(3) Chernikova, A.; Kozodaev, M.; Markeev, A.; Matveev, Y.; Negrov, D.; Orlov, O. Confinement-free annealing induced ferroelectricity in $Hf_{0.5}Zr_{0.5}O_2$ thin films. *Microelectron. Eng.* **2015**, *147*, 15−18.

(4) Böscke, T. S.; Müller, J.; Bräuhaus, D.; Schröder, U.; Böttger, U. Ferroelectricity in hafnium oxide thin films. *Appl. Phys. Lett.* **2011**, *99*, 102903.

(5) Starschich, S.; Boettger, U. An extensive study of the influence of dopants on the ferroelectric properties of HfO_2. *J. Mater. Chem. C* **2017**, *5*, 333−338.

(6) Park, M. H.; Lee, Y. H.; Kim, H. J.; Kim, Y. J.; Moon, T.; Kim, K. D.; Müller, J.; Kersch, A.; Schroeder, U.; Mikolajick, T.; Hwang, C. S. Ferroelectricity and Antiferroelectricity of Doped Thin HfO_2-Based Films. *Adv. Mater.* **2015**, *27*, 1811−1831.

(7) Mattinen, M.; Hämäläinen, J.; Vehkamäki, M.; Heikkilä, M. J.; Mizohata, K.; Jalkanen, P.; Räisänen, J.; Ritala, M.; Leskelä, M. Atomic Layer Deposition of Iridium Thin Films Using Sequential Oxygen and Hydrogen Pulses. *J. Phys. Chem. C* **2016**, *120*, 15235−15243.

(8) Egorov, K. V.; Lebedinskii, Y. Y.; Soloviev, A. A.; Chouprik, A. A.; Azarov, A. Y.; Markeev, A. M. Initial and steady-state Ru growth by atomic layer deposition studied by in situ Angle Resolved X-ray Photoelectron Spectroscopy. *Appl. Surf. Sci.* **2017**, *419*, 107−113.

(9) Park, M. H.; Kim, H. J.; Kim, Y. J.; Moon, T.; Kim, K. D.; Lee, Y. H.; Hyun, S. D.; Hwang, C. S. Study on the internal field and conduction mechanism of atomic layer deposited ferroelectric $Hf_{0.5}Zr_{0.5}O_2$ thin films. *J. Mater. Chem. C* **2015**, *3*, 6291−6300.

(10) Zarubin, S.; Suvorova, E.; Spiridonov, M.; Negrov, D.; Chernikova, A.; Markeev, A.; Zenkevich, A. Fully ALD-grown TiN/$Hf_{0.5}Zr_{0.5}O_2$/TiN stacks: Ferroelectric and structural properties. *Appl. Phys. Lett.* **2016**, *109*, 192903.

(11) Park, I.-S.; Ryu, K.-m.; Jeong, J.; Ahn, J. Dielectric stacking effect of Al_2O_3 and HfO_2 in metal−insulator−metal capacitor. *IEEE Electron Device Lett.* **2013**, *34*, 120−122.

(12) Materlik, R.; Künneth, C.; Kersch, A. The origin of ferroelectricity in $Hf_{1-x}Zr_xO_2$: A computational investigation and a surface energy model. *J. Appl. Phys.* **2015**, *117*, 134109.

(13) Huan, T. D.; Sharma, V.; Rossetti, G. A., Jr.; Ramprasad, R. Pathways towards ferroelectricity in hafnia. *Phys. Rev. B: Condens. Matter Mater. Phys.* **2014**, *90*, 064111.

(14) Park, M. H.; Lee, Y. H.; Kim, H. J.; Kim, Y. J.; Moon, T.; Kim, K. D.; Hyun, S. D.; Mikolajick, T.; Schroeder, U.; Hwang, C. S. Understanding the formation of the metastable ferroelectric phase in hafnia−zirconia solid solution thin films. *Nanoscale* **2018**, *10*, 716−725.

(15) Zhang, H.; Gao, B.; Yu, S.; Lai, L.; Zeng, L.; Sun, B.; Liu, L.; Liu, X.; Lu, J.; Han, R.; Kang, J. Effects of ionic doping on the behaviors of oxygen vacancies in HfO_2 and ZrO_2: A first principles study. *International Conference on Simulation of Semiconductor Processes and Devices (SISPAD)*, 2009.

(16) Muller, J.; Boscke, T. S.; Muller, S.; Yurchuk, E.; Polakowski, P.; Paul, J.; Martin, D.; Schenk, T.; Khullar, K.; Kersch, A.; Weinreich, W.; Riedel, S.; Seidel, K.; Kumar, A.; Arruda, T. M.; Kalinin, S. V.; Schlosser, T.; Boschke, R.; van Bentum, R.; Schroder, U.; Mikolajick, T. Ferroelectric hafnium oxide: A CMOS-compatible and highly scalable approach to future ferroelectric memories. *Electron Devices Meeting (IEDM)*; IEEE International: Washington, 2013; pp 10.8.1−10.8.4.

(17) Chernikova, A. G.; Kuzmichev, D. S.; Negrov, D. V.; Kozodaev, M. G.; Polyakov, S. N.; Markeev, A. M. Ferroelectric properties of full plasma-enhanced ALD TiN/La:HfO_2/TiN stacks. *Appl. Phys. Lett.* **2016**, *108*, 242905.

(18) Duran, P. Phase relationships in the systems HfO_2-La_2O_3 and HfO_2-Nd_2O_3. *Ceram. Int.* **1975**, *1*, 10−13.

(19) Ushakov, S. V.; Brown, C. E.; Navrotsky, A. Effect of La and Y on Crystallization Temperatures of Hafnia and Zirconia. *J. Mater. Res.* **2004**, *19*, 693−696.

(20) Kozodaev, M. G.; Lebedinskii, Y. Y.; Chernikova, A. G.; Polyakov, S. N.; Markeev, A. M. Low temperature plasma-enhanced ALD TiN ultrathin films for $Hf_{0.5}Zr_{0.5}O_2$-based ferroelectric MIM structures. *Phys. Status Solidi A* **2017**, *214*, 1700056.

(21) Park, M. H.; Schenk, T.; Fancher, C. M.; Grimley, E. D.; Zhou, C.; Richter, C.; LeBeau, J. M.; Jones, J. L.; Mikolajick, T.; Schroeder, U. A comprehensive study on the structural evolution of HfO_2 thin films doped with various dopants. *J. Mater. Chem. C* **2017**, *5*, 4677−4690.

(22) Chernikova, A.; Kozodaev, M.; Markeev, A.; Negrov, D.; Spiridonov, M.; Zarubin, S.; Bak, O.; Buragohain, P.; Lu, H.; Suvorova, E.; Gruverman, A.; Zenkevich, A. Ultrathin $Hf_{0.5}Zr_{0.5}O_2$ Ferroelectric Films on Si. *ACS Appl. Mater. Interfaces* **2016**, *8*, 7232−7237.

(23) Chouprik, A.; Chernikova, A.; Markeev, A.; Mikheev, V.; Negrov, D.; Spiridonov, M.; Zarubin, S.; Zenkevich, A. Electron transport across ultrathin ferroelectric $Hf_{0.5}Zr_{0.5}O_2$ films on Si. *Microelectron. Eng.* **2017**, *178*, 250−253.

(24) Islamov, D. R.; Chernikova, A. G.; Kozodaev, M. G.; Markeev, A. M.; Perevalov, T. V.; Gritsenko, V. A.; Orlov, O. M. Charge transport mechanism in thin films of amorphous and ferroelectric $Hf_{0.5}Zr_{0.5}O_2$. *JETP Lett.* **2015**, *102*, 544−547.

(25) Nečas, D.; Klapetek, P. Gwyddion: an open-source software for SPM data analysis. *Cent. Eur. J. Phys.* **2012**, *10*, 181−188.

(26) Kozodaev, M. G.; Chernikova, A. G.; Korostylev, E. V.; Park, M. H.; Schroeder, U.; Hwang, C. S.; Markeev, A. M. Ferroelectric properties of lightly doped La:HfO_2 thin films grown by plasma-assisted atomic layer deposition. *Appl. Phys. Lett.* **2017**, *111*, 132903.

(27) Preisach, F. Über die Magnetische Nachwirkung. *Z. Phys.* **1935**, *94*, 277−302.

(28) Pešić, M.; Fengler, F. P. G.; Larcher, L.; Padovani, A.; Schenk, T.; Grimley, E. D.; Sang, X.; LeBeau, J. M.; Slesazeck, S.; Schroeder, U.; Mikolajick, T. Physical Mechanisms behind the Field-Cycling Behavior of HfO_2-based Ferroelectric Capacitors. *Adv. Funct. Mater.* **2016**, *26*, 4601−4612.

(29) Schenk, T.; Hoffmann, M.; Ocker, J.; Pešić, M.; Mikolajick, T.; Schroeder, U. Complex Internal Bias Fields in Ferroelectric Hafnium Oxide. *ACS Appl. Mater. Interfaces* **2015**, *7*, 20224−20233.

(30) Grimley, E. D.; Schenk, T.; Sang, X.; Pešić, M.; Schroeder, U.; Mikolajick, T.; LeBeau, J. M. Structural changes Underlying Field-Cycling Phenomena in Ferroelectric HfO_2 thin films. *Adv. Electron. Mater.* **2016**, *2*, 1600173.

(31) Warren, W. L.; Dimos, D.; Tuttle, B. A.; Nasby, R. D.; Pike, G. E. Electronic domain pinning in Pb(Zr,Ti)O_3 thin films and its role in fatigue. *Appl. Phys. Lett.* **1994**, *65*, 1018.

(32) Richter, C.; Schenk, T.; Park, M. H.; Tscharntke, F. A.; Grimley, E. D.; LeBeau, J. M.; Zhou, C.; Fancher, C. M.; Jones, J. L.; Mikolajick, T.; Schroeder, U. Si Doped Hafnium Oxide-A "Fragile" Ferroelectric System. *Adv. Electron. Mater.* **2017**, *3*, 1700131.

(33) Gao, B.; Zhang, H. W.; Yu, S.; Sun, B.; Liu, L. F.; Liu, X. Y.; Wang, Y.; Han, R. Q.; Kang, J. F.; Yu, B.; Wang, Y. Y. Oxide-Based RRAM: Uniformity Improvement Using A New Material-Oriented Methodology. *Digest of Technical Papers—Symposium on VLSI Technology*, Kyoto, 2009; pp 30−31.

DOI: 10.1021/acsami.7b15110
ACS Appl. Mater. Interfaces XXXX, XXX, XXX−XXX